Article

UV Raman Demonstrates that α-Helical Polyalanine Peptides Melt to Polyproline II Conformations

Sanford A. Asher, Alexander V. Mikhonin, and Sergei Bykov

J. Am. Chem. Soc., **2004**, 126 (27), 8433-8440• DOI: 10.1021/ja049518j • Publication Date (Web): 19 June 2004

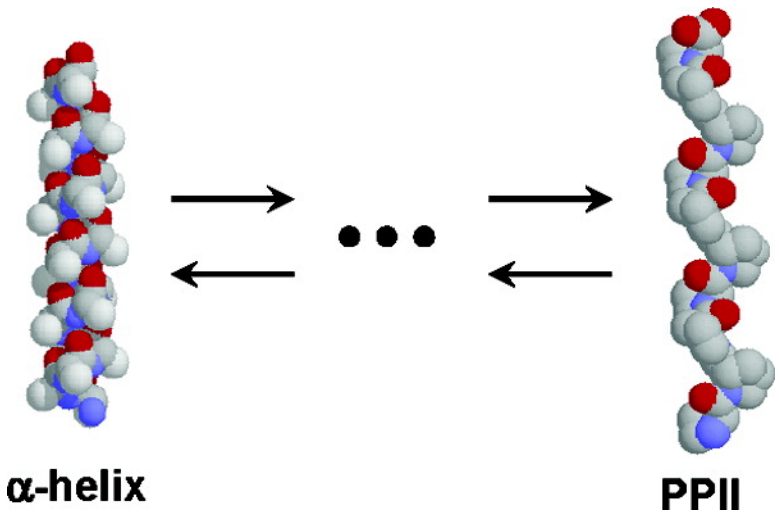

J|A|C|S
ARTICLES
Published on Web 06/19/2004

UV Raman Demonstrates that α-Helical Polyalanine Peptides Melt to Polyproline II Conformations

Sanford A. Asher,* Alexander V. Mikhonin, and Sergei Bykov

Contribution from the Department of Chemistry, University of Pittsburgh, Pittsburgh, Pennsylvania 15260

Received January 27, 2004; E-mail: asher@pitt.edu

Abstract: We examined the 204-nm UV Raman spectra of the peptide XAO, which was previously found by Shi et al.'s NMR study to occur in aqueous solution in a polyproline II (PPII) conformation (*Proc. Natl. Acad. Sci. U.S.A.* **2002**, *99*, 9190). The UV Raman spectra of XAO are essentially identical to the spectra of small peptides such as ala_5 and to the large 21-residue predominantly Ala peptide, AP. We conclude that the non-α-helical conformations of these peptides are dominantly PPII. Thus, AP, which is highly α-helical at room temperature, melts to a PPII conformation. There is no indication of any population of intermediate disordered conformations. We continued our development of methods to relate the Ramachandran Ψ-angle to the amide III band frequency. We describe a new method to estimate the Ramachandran Ψ-angular distributions from amide III band line shapes measured in 204-nm UV Raman spectra. We used this method to compare the Ψ-distributions in XAO, ala_5, the non-α-helical state of AP, and acid-denatured apomyoglobin. In addition, we estimated the Ψ-angle distributions of peptide bonds which occur in non-α-helix and non-β-sheet conformations in a small library of proteins.

Introduction

The classical view of protein structure and function is that a native protein structure is defined by a single conformation or by a restricted subset of similar conformations, which occur at the minimum (or one of the minima) of the conformational protein energy landscape.[1−7] For many proteins, the native structure is defined as the conformation that an isolated denatured protein evolves into when the chemical environment is altered to favor folding.[8−12] The denatured states are much less defined,[9,13−16] with the likelihood that numerous states are involved, in particular subsets of which are favored by different denaturing environmental conditions. These conformational subsets, as sampled by the peptide bond conformations, are expected to be much smaller than those conformations possible by simply excluding the sterically disallowed peptide bond dihedral angles, which occur in the forbidden portions of the Ramachandran plot.[17] The conformational subspace(s) of the amide bonds of denatured proteins is also expected to be much smaller than the conformational subspace which would remain by additionally excluding all sterically problematic side chain conformations.[18]

The term "denatured" or "non-native" state is generally used to denote a variety of protein-unfolded states which conformationally differ from that of the biologically active native state. Care is necessary when using these definitions, since unfolded states may have biological function.[19,20] In many cases, the denatured structure is expected to have a random secondary structure where the backbone randomly adopts energetically allowed Ψ- and Φ-Ramachandran angles, since it has been thought, until recently, that conformational correlations should not exist between adjacent peptide bonds.[21] In this case, for a random coil peptide sequence there would be no correlation in peptide bond conformations between adjacent or distant peptide bonds. It should be mentioned, however, that this assumption has been recently questioned.[22−27]

(1) Chan, H. S.; Dill, K. A. *Proteins: Struct., Funct., Genet.* **1998**, *30*, 2−33.
(2) Dill, K. A. *Biochemistry* **1990**, *29*, 7133−7155.
(3) Pokarowski, P.; Kolinski, A.; Skolnick, J. *Biophys. J.* **2003**, *84*, 1518−1526.
(4) Jewett, A. I.; Pande, V. S.; Plaxco, K. W. *J. Mol. Biol.* **2003**, *326*, 247−253.
(5) Hardin, C.; Eastwood, M. P.; Prentiss, M.; Luthey-Schulten, Z.; Wolynes, P. G. *J. Comput. Chem.* **2002**, *23*, 138−146.
(6) Alm, E.; Baker, D. *Proc. Natl. Acad. Sci. U.S.A.* **1999**, *96*, 11305−11310.
(7) Socci, N. D.; Onucic, J. N.; Wolynes, P. G. *Proteins: Struct., Funct., Genet.* **1998**, *32*, 136−158.
(8) Anfinsen, C. B. *Science* **1973**, *181*, 223−230.
(9) Mayor, U.; Guydosh, N. R.; Johnson, C. M.; Grossmann, J. G.; Sato, S.; Jas, G. S.; Freund, S. M. V.; Alonso, D. O. V.; Daggett, V.; Fersht, A. R. *Nature* **2003**, *421*, 863−867.
(10) Myers, J. K.; Oas, T. G. *Annu. Rev. Biochem.* **2002**, *71*, 783−815.
(11) Mirny, L.; Shakhnovich, E. *Annu. Rev. Biophys. Biomol. Struct.* **2001**, *30*, 361−396.
(12) Englander, S. W. *Annu. Rev. Biophys. Biomol. Struct.* **2000**, *29*, 213−238.
(13) Shortle, D. *Curr. Opin. Struct. Biol.* **1993**, *3*, 66−74.
(14) Daura, X.; Glattli, A.; Gee, P.; Peter, C.; Van Gunsteren, W. F. *Adv. Prot. Chem.* **2002**, *62*, 341−360.
(15) Van Gunsteren, W. F.; Burgi, R.; Peter, C.; Daura, X. *Angew. Chem., Int. Ed.* **2001**, *40*, 352−355.
(16) Fiebig, K. M.; Schwalbe, H.; Buck, M.; Smith, L. J.; Dobson, C. M. *J. Phys. Chem.* **1996**, *100*, 2661−2666.
(17) Ramachandran, G. N.; Sasisekharan, V. *Adv. Protein Chem.* **1968**, *23*, 283−438.
(18) Shortle, D. *Protein Sci.* **2002**, *11*, 18−26.
(19) Gast, K.; Damaschun, H.; Eckert, K.; Schulze-Forster, K.; Maurer, H. R.; Mueller-Frohne, M.; Zirwer, D.; Czarnecki, J.; Damaschun, G. *Biochemistry* **1995**, *34*, 13211−13218.
(20) Penkett, C. J.; Redfield, C.; Jones, J. A.; Dodd, I.; Hubbard, J.; Smith, R. A.; Smith, L. J.; Dobson, C. M. *Biochemistry* **1998**, *37*, 17054−17067.
(21) Flory, P. J. *Statistical Mechanics of Chain Molecules*; Interscience Publishers: New York, 1969.
(22) Pappu, R. V.; Srinivasan, R.; Rose, G. D. *Proc. Natl. Acad. Sci. U.S.A.* **2000**, *97*, 12565−12570.

Evidence has recently been presented which indicates that even small peptides have defined solution backbone conformations and that the "random coil conformation" approximation is invalid even for small peptides such as dialanine.[28,29] These new data have resurrected the early arguments by Tiffany and Krimm[30] that CD spectra indicate a nonrandom secondary structure for polyglutamic acid and polylysine peptides, whose structure was proposed to resemble the polyproline II-type helical structure (PPII helix, or 3_1-helix). This PPII left-handed backbone helical structure shows Ψ- and Φ-angles of 145° and −75°, respectively, with three residues per helical turn.

The unfolded states of other small peptides such as ala_3 (A_3),[31,32] A_7,[33] K_7,[34] and much larger peptides such as poly-L-lysine,[35,36] poly-L-glutamic acid[35,36] and poly-L-glutamate,[36] and poly-L-aspartate peptides[36] have also been reported to adopt locally ordered PPII helical conformations.

Evidence for local order has also appeared in VCD studies of high molecular weight poly-L-lys and poly-L-glutamic acid.[37] In addition, researchers have recently presented evidence that the so-called unordered regions of native proteins contain a considerable amount of PPII structure.[35,38−40] The recent excellent reviews discussing PPII conformations by Shi et al.[41] and Bochicchio et al.[42] should also be consulted for recent views regarding the importance of the PPII structure. In addition, Blanch et al.[43] recently used Raman optical activity to examine melting of lysozymes and a 21-amino acid alanine-rich peptide and found evidence for melting to a PPII conformation.

In this work, we used UV Raman spectroscopy[44,45] to examine the melting of a 21-residue A-based peptide AAAAA-$(AAARA)_3$A (AP) which contains three R to confer solubility.[46,47] We find that the melting occurs from an α-helix to a mainly PPII conformation. We find no evidence for a "random coil" conformation. The fact that the melting involves a transition mainly between two defined conformations calls into question the validity of the models[48,49] typically used to model α-helix folding and unfolding. These models assume a large entropic penalty for α-helix nucleation, since they imagine that the nucleus requires the conformational constraint of four residues from a high-entropy random coil conformational state to begin the growth of longer α-helices. It appears that the α-helix nucleation is not as entropically expensive as proposed, since the conformational change involves transitions between restricted peptide conformational subspaces, between the PPII state(s) to the α-helix-like nucleus. These considerations may dramatically change modeling of the folding and unfolding of α-helices, at least for AP-type peptides.

Experimental Section

Sample Preparation. The 21-residue alanine-based peptide AAAAA-$(AAARA)_3$A (AP) was prepared (HPLC pure) at the Pittsburgh Peptide Facility by using the solid-state peptide synthesis method. The AP solutions in water contained 1 mg/mL concentrations of AP and 0.2 M concentrations of sodium perchlorate, which were used as internal intensity and frequency standards.[46,47] All Raman spectra were normalized to the intensity of the ClO_4^- Raman band (932 cm^{-1}).

A_5 and A_3 peptides were purchased from Bachem Bioscience, Inc. (King of Prussia, PA) and used as received. The $A_5 - A_3$ Raman difference spectral measurements utilized identical molar concentrations of A_5 and A_3 (0.34 mg/mL and 0.2 mg/mL, respectively) in solutions containing identical sodium perchlorate concentrations (0.2 M). We normalized the Raman spectra to the intensity of the 932 cm^{-1} perchlorate internal standard band. The $A_5 - A_3$ difference spectra were calculated by subtracting the normalized A_3 spectrum from the normalized A_5 spectrum at each temperature.

The undecapeptide XAO (MW = 985) was prepared (HPLC pure) at the Pittsburgh Peptide Facility by using the solid-state peptide synthesis method. The sequence of this peptide is Ac-XXAAAAAAAOO-amide, where all amino acids are in their L form, and A is alanine, X is diaminobutyric acid (side chain $CH_2CH_2NH_3^+$), and O is ornithine (side chain $(CH_2)_3NH_3^+$). We used 1 mg/mL solutions of XAO peptide containing 0.15 M sodium perchlorate. The UVRR spectra of XAO were also normalized to the ClO_4^- Raman band intensity.

Horse heart metmyoglobin (holoMb) was purchased from Sigma Chemical Co. (St. Louis, MO). ApoMb was made by a 2-butanone extraction of the heme using the procedure of Teale,[50] followed by Sephedex-25 gel chromatography. Absorption measurements indicated that >99% of the heme was removed. The apoMb was lyophilized and stored at −20 °C. We used 200 μM apoMb solutions (~3 mg/mL) for the steady-state Raman measurements. The apoMb sample pH was adjusted to the desired value (pH = 1.86) by using HCl. Concentrations were determined from UV absorption spectra by using a molar absorptivity of 14,260 M^{-1} cm^{-1} at 280 nm.[51,52]

Instrumentation. The UV Resonance Raman instrumentation has been described in detail elsewhere.[46,47] A Coherent Infinity Nd:YAG laser produced 355 nm (3rd harmonic), 3 ns pulses at 100 Hz. This beam was Raman-shifted to 204 nm (fifth anti-Stokes) by using a 1-m tube filled with hydrogen (60 psi). A Pellin Broca prism was used to select the 204-nm excitation beam. The Raman scattered light was imaged into a subtractive double spectrometer,[53] and the UV light was detected by either a Princeton Instruments solar blind ICCD camera or

(23) Srinivasan, R.; Rose, G. D. *Proc. Natl. Acad. Sci. U.S.A.* **1999**, *96*, 14258−14263.
(24) Marqusee, S.; Robbins, V. H.; Baldwin, R. L. *Proc. Natl. Acad. Sci. U.S.A.* **1989**, *86*, 5286−5290.
(25) Pal, D.; Suhnel, J.; Weiss, M. S. *Angew. Chem., Int. Ed.* **2002**, *41*, 4663−4665.
(26) Watson, J. D.; Milner-White, E. J. *J. Mol. Biol.* **2002**, *315*, 171−182.
(27) Watson, J. D.; Milner-White, E. J. *J. Mol. Biol.* **2002**, *315*, 183−191.
(28) Gnanakaran, S.; Hochstrasser, R. M. *J. Am. Chem. Soc.* **2001**, *123*, 12886−12898.
(29) Schweitzer-Stenner, R.; Eker, F.; Huang, Q.; Griebenow, K.; Mroz, P. A.; Kozlowski, P. M. *J. Phys. Chem. B* **2002**, *106*, 4294−4304.
(30) Tiffany, M. L.; Krimm, S. *Biopolymers* **1968**, *6*, 1379−1382.
(31) Woutersen, S.; Hamm, P. *J. Phys. Chem. B* **2000**, *104*, 11316−11320.
(32) Eker, F.; Cao, X.; Nafie, L.; Schweitzer-Stenner, R. *J. Am. Chem. Soc.* **2002**, *124*, 14330−14341.
(33) Shi, Z.; Olson, C. A.; Rose, G. D.; Baldwin, R. L.; Kallenbach, N. R. *Proc. Natl. Acad. Sci. U.S.A.* **2002**, *99*, 9190−9195.
(34) Rucker, A. L.; Creamer, T. P. *Protein Sci.* **2002**, *11*, 980−985.
(35) Smyth, E.; Syme, C. D.; Blanch, E. W.; Hecht, L.; Vasak, M.; Barron, L. D. *Biopolymers* **2001**, *58*, 138−151.
(36) Woody, R. W. *Adv. Biophys. Chem.* **1992**, *2*, 37−79.
(37) Keiderling, T. A.; Silva, R. A.; Yoder, G.; Dukor, R. K. *Bioorg. Med. Chem.* **1999**, *7*, 133−141.
(38) Adzhubei, A. A.; Sternberg, M. J. E. *J. Mol. Biol.* **1993**, *229*, 472−493.
(39) Syme, C. D.; Blanch, E. W.; Holt, C.; Jakes, R.; Goedert, M.; Hecht, L.; Barron, L. D. *Eur. J. Biochem.* **2002**, *269*, 148−156.
(40) Sreerama, N.; Woody, R. W. *Biochemistry* **1994**, *33*, 10022−10025.
(41) Shi, Z.; Woody, R. W.; Kallenbach, N. R. *Adv. Prot. Chem.* **2002**, *62*, 163−240.
(42) Bochicchio, B.; Tamburro, A. M. *Chirality* **2002**, *14*, 782−792.
(43) Blanch, E. W.; Morozova-Roche, L. A.; Cochran, D. A. E.; Doig, A. J.; Hecht, L.; Barron, L. D. *J. Mol. Biol.* **2000**, *301*, 553−563.
(44) Asher, S. A. *Anal. Chem.* **1993**, *65*, 59A-66A, 201A-210A.
(45) Asher, S. A. In *Handbook of Vibrational Spectroscopy*; Chalmers, J. M., Griffiths, P. R., Eds.; John Wiley & Sons: New York, 2002; pp 557−571.
(46) Lednev, I. K.; Karnoup, A. S.; Sparrow, M. C.; Asher, S. A. *J. Am. Chem. Soc.* **1999**, *121*, 8074−8086.
(47) Lednev, I. K.; Karnoup, A. S.; Sparrow, M. C.; Asher, S. A. *J. Am. Chem. Soc.* **2001**, *123*, 2388−2392.
(48) Lifson, S.; Roig, A. *J. Chem. Phys.* **1961**, *34*, 1963−1974.
(49) Zimm, B. H.; Bragg, J. K. *J. Chem. Phys.* **1959**, *31*, 526−535.
(50) Teale, F. W. J. *Biochim. Biophys. Acta* **1959**, *35*, 543.
(51) Longworth, J. W. In *Excited States of Proteins and Nucleic Acids*; Steiner, R. F., Weinryb, I., Eds.; Plenum Press: New York, 1971; pp 319−484.
(52) Edelhoch, H. *Biochemistry* **1967**, *6*, 1948−1954.
(53) Asher, S. A. In preparation, 2004.

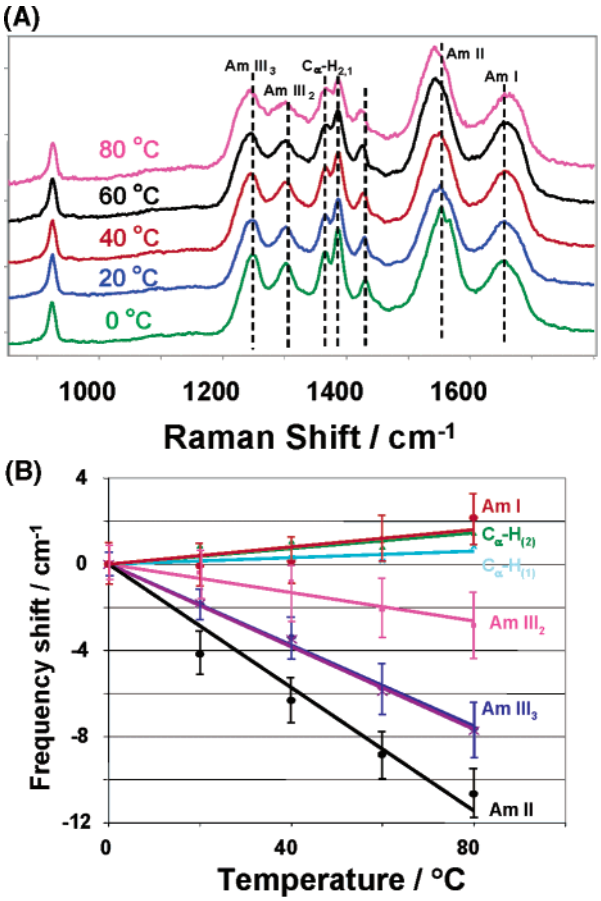

Figure 1. (A) 204-nm UVRR spectra of PPII helical XAO peptide at 0, +20, +40, +60, and +80 °C. (B) Temperature dependence of PPII helix UVRR bands. The contribution of the broad water bending band centered at ~1630 cm^{-1} and the sharp O_2 stretching band at 1556 cm^{-1} have been numerically removed.

a Roper Scientific unintensified, back-thinned, liquid nitrogen-cooled CCD camera. All samples were measured in a thermostated free surface flow stream.

Results and Discussion

UV Raman Spectra of PPII XAO Indicate that Melted AP Is in a PPII Conformation. Shi et al.[33] carefully measured the temperature dependence of the NMR spectra of XAO peptide and definitively showed that at 2 °C the structure in water was mainly PPII helix (with no more than 10% β-strand). The structure remained dominantly PPII helix at 52 °C, with a ~12% increase in β-strand concentration. We compared the UV resonance Raman spectrum of XAO to the melted form of AP, a 21-amino acid mainly Ala peptide. Figure 1 shows the 204 nm UV Raman spectra of XAO peptide between 0 and 80 °C. Excitation (204 nm) occurs within the $\pi \rightarrow \pi^*$ transitions of the amide peptide bonds.[54] Excitation into these electronic transitions mainly enhances the vibrations of the amide backbone.[55−58]

The XAO UV Raman spectra are essentially invariant with temperature. At 20 °C the spectra[46,47] show the AmI band (~1657 cm^{-1}, mainly C═O stretching of the peptide bond), the AmII band (~1550 cm^{-1}, CN stretch and NH bending), and the C_α−H sb doublet (~1388 and 1365 cm^{-1}, a symmetric bending vibration which is enhanced because of coupling with the AmIII vibration). The amide III spectral region is very complex[59−62] and normally is considered to have a number of contributing bands which also derive from CN stretch and NH bending as well as other amide coordinates. We will elucidate the detailed assignments of these bands in a forthcoming publication,[63] but here we enumerate only two of the important amide III region bands: the $AmIII_2$ (~1302 cm^{-1}) and the $AmIII_3$ (~1244 cm^{-1}) bands.[64]

The frequency of the amide III bands and the resonance Raman enhancement of the C_α−H sb bands depend mainly on the degree of coupling between C_α−H sb and N−H sb motions, which strongly depends on the amide bond Ψ-angle.[65] The lowest amide III_3 band frequencies and the strongest mixing were originally expected[65] at $\Psi \approx 180°$, where the C_α−H and N−H bonds are cis. In contrast, essentially no mixing occurs for $\Psi = -60°$ (α-helix Ψ-angle), where the C_α−H and N−H bonds are trans.[65]

The low frequency of the amide III bands and the strong enhancement of the C_α−H sb vibration in XAO are fully consistent[65] with the PPII conformation ($\Psi \approx 145°$) determined by NMR. However, this low frequency could also be consistent with a β-strand conformation. The lack of a temperature dependence of the UV Raman spectra, except for the small monotonic frequency shifts[46] discussed below in detail, indicates a single, essentially invariant secondary structure conformation.

The band positions and the spectral shape of the XAO UV Raman spectra are very similar to those observed for the unfolded state of the ala-based AP peptide (Figure 2) and the $A_5 - A_3$ difference spectra.[46] The main difference is that the XAO peptide spectrum shows a decreased $AmIII_3$ frequency (1240 cm^{-1} at +60 °C) and a smaller relative intensity compared to both AP (1247 cm^{-1} at +62 °C) and $A_5 - A_3$ (1250 cm^{-1} at +50 °C). This frequency shift could result from small differences in the Ψ-angles from their normal PPII values of 145°.

Asher et al.'s study[65] of the Ψ- and Φ-dependence of the AmIII vibrational frequencies exposed the simple relationship: $\upsilon \approx \upsilon_o + A \sin(\Psi - \delta)$, where υ is the calculated AmIII frequency, υ_o is the AmIII frequency baseline, A is the amplitude of the frequency dependence on Ψ, and δ is the relative phase of the sine curve with respect to Ψ. As discussed below (eq 2), we have fit this relationship to new solution and crystal Raman data and found that this 7 cm^{-1} frequency increase in AP could result from a ~10° increase to $\Psi = 155°$.

It is, however, more likely that the spectral differences between AP and XAO derive from the ~50% XAO amide bonds contributed by non-ala amino acids, which are likely to influence

(54) Robin, M. B. *Higher Excited States of Polyatomic Molecules*; Academic Press: New York, 1975; Vol. II.
(55) Song, S.; Asher, S. A. *J. Am. Chem. Soc.* **1989**, *111*, 4295−4305.
(56) Dudik, J. M.; Johnson, C. R.; Asher, S. A. *J. Phys. Chem.* **1985**, *89*, 3805−3814.
(57) Copeland, R. A.; Spiro, T. G. *Biochemistry* **1987**, *26*, 2134.
(58) Mayne, L. C.; Ziegler, L. D.; Hudson, B. *J. Phys. Chem.* **1985**, *89*, 3395.
(59) Oboodi, M. R.; Alva, C.; Diem, M. *J. Phys. Chem.* **1984**, *88*, 501−505.
(60) Diem, M.; Lee, O.; Roberts, G. M. *J. Phys. Chem.* **1992**, *96*, 548−554.
(61) Lee, S. H.; Krimm, S. *Biopolymers* **1998**, *46*, 283−317.
(62) Overman, S. A.; Thomas, G. J., Jr. *Biochemistry* **1998**, *37*, 5654−5665.
(63) Mikhonin, A. V.; Ahmed, Z.; Ianoul, A.; Asher., S. A. In preparation, 2004.
(64) The number scheme used here is consistent with that which we will use in a forthcoming article,[63] which examines the assignment of all bands in the amide III region of PPII and α-helix peptides. The subscripts enumerate from highest frequency to lowest frequency as typical for vibration-mode labeling. Unfortunately, this is the opposite of Diem et al.'s[60] labeling scheme. The amide III_1 band is not discussed in this article.
(65) Asher, S. A.; Ianoul, A.; Mix, G.; Boyden, M. N.; Karnoup, A.; Diem, M.; Schweitzer-Stenner, R. *J. Am. Chem. Soc.* **2001**, *123*, 11775−11781.

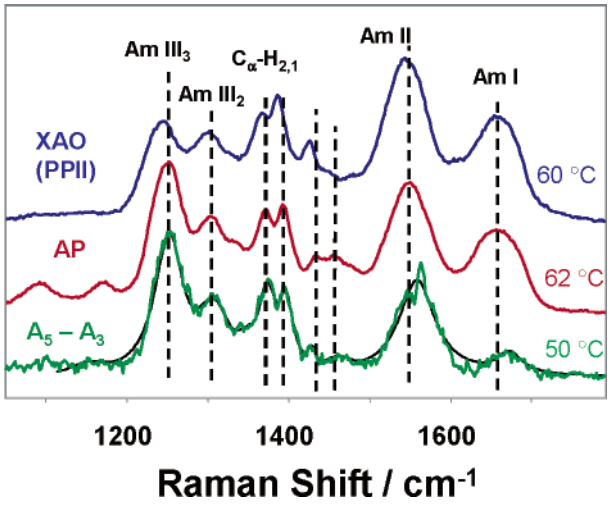

Figure 2. Comparison of 204-nm Raman spectra of predominantly PPII helical XAO peptide at +60 °C to that of non-α-helical AP at +62 °C, and $A_5 - A_3$ at +50 °C.

the Φ-angle as shown by Ianoul et al.[66] This could decrease their $AmIII_3$ frequencies, which would broaden the band and decrease the peak height as observed here. Mirkin and Krimm[67] also demonstrated that the AmIII frequency depends on both the Ψ- and Φ-angles rather than the Ψ-angle alone.[68]

The temperature dependence of the XAO UV Raman band frequencies (Figure 1) is essentially identical to that of AP (within experimental precision,[46] Table 1). The XAO AmII band shows a -0.14 cm^{-1}/K temperature coefficient, while the $AmIII_3$ band shows a somewhat smaller -0.10 cm^{-1}/K coefficient, as shown in Table 1. The $C_\alpha-H$ bending shows no temperature dependence (within experimental error), while the AmI bands show small positive coefficients.

As discussed in detail elsewhere,[69,70] this spectral dependence derives from a weakening of the hydrogen bonding of water to the amide carbonyl and N−H groups. The hydrogen-bonding coordinate is anharmonic, which results in an increased water-to-amide hydrogen bond length as the temperature increases (Figure 3). The consequent decrease in hydrogen bond strength increases the contribution of the Figure 3b resonance form, which would decrease the AmII and AmIII band frequencies and would increase the AmI band frequency, as observed.

The identical amide band frequency temperature dependencies for AP, $A_5 - A_3$, and XAO clearly indicate essentially identical exposures to water and identical backbone hydrogen bonding to water. *All of these results force us to conclude that non-α-helical AP and the inner peptide bonds of A_5 occur in PPII-like conformations.* Although we find that non-α-helical AP occurs in a predominantly PPII helix conformation, this does not mean that the PPII helix conformation spans the entire AP length. Rather, it is more likely that stretches of PPII helix occur which are separated by *β*-turns, for example.

AP Melts from an α-Helix to a Mainly PPII Conformation. The Figure 4 temperature difference spectra between 60 °C and 0 °C for XAO and non-α-helical AP peptides are very similar. This AP difference spectrum was modeled from Lednev et al.'s data[46] by numerically removing the α-helix contribution from the 0 °C AP spectrum.

AP is 55% α-helical at 0 °C. The helix melts as the temperature increases. Lednev et al.'s kinetic measurements[46,47] showed that α-helical AP melts in the ∼200-ns time regime following 3-ns T-jumps. They found that the transient AP difference spectra at the shortest (∼14 ns) times look identical to the equilibrium temperature difference spectra for the non-α-helical form of AP between the two temperatures (compare Figure 4 to Figure 3 of Lednev et al.[47]). Thus, these spectral changes were interpreted to result from the T-induced difference spectra of the "disordered" form of AP, which we can now ascribe to the mainly PPII conformations of a fraction of the AP chains. Only at times >50 ns do spectral changes appear, which indicate melting of α-helices to a conformation which is predominantly PPII. We see no evidence of any additional intermediate conformations. Whatever the reaction pathway, the melting from α-helix to PPII is fast.

Temperature Dependence of Amide Frequencies. Recent studies have also demonstrated that small peptides adopt the PPII structure in solution.[31−33] Figure 5 shows the temperature dependence of the Raman difference spectra between Ala_5 and Ala_3 ($A_5 - A_3$). This difference spectrum removes the spectral contributions of the penultimate amide bonds and allows us to concentrate on the two central amide bonds of Ala_5. As noted by Lednev et al.,[46] these $A_5 - A_3$ spectra are very close to the spectra of non-α-helical AP (PPII structure). In fact, they show the same temperature dependence of the amide frequencies. This allows us to conclude that the interior amide bonds of Ala_5 are predominantly in a PPII conformation.

A similar PPII-type spectrum can also be obtained from proteins denatured at low pH. For example, Figure 6 shows the 204-nm UV Raman spectra of apoMb at pH = 1.86 and +25 °C (<20% α-helix). Essentially, all α-helices have melted. The unfolded apoMb spectrum is close to that of XAO and AP, suggesting a significant population of the PPII conformation in this unfolded protein. However, the amide bands are broad, and the higher frequency $AmIII_3$ shoulder indicates additional contributions from non-PPII conformations.

Frequency Dependence of Disordered Peptide Bonds of Folded Proteins. The UV Raman spectra of "disordered segments" of folded proteins show little evidence of PPII conformations. Figure 6 shows the UV Raman basis spectrum of the disordered conformations of the library of native proteins measured by Chi et al.[71] The UV Raman spectra from this protein library were found to have three main factors which completely determined its spectral features: the α-helix, *β*-sheet, and "unordered" forms. Since the conformations of all of these proteins were known from X-ray diffraction, we were able to calculate the basis spectra of the three contributing secondary structure motifs: the α-helix, *β*-sheet, and "unordered" conformations of these folded proteins.

The UV Raman basis spectrum of the "disordered" peptide bonds is extremely broad. For example, the AmIII band spans the 1220−1320 cm^{-1} spectral region. This frequency span is likely to result from a subset of amide bonds with Ψ- and

(66) Ianoul, A.; Boyden, M. N.; Asher, S. A. *J. Am. Chem. Soc.* **2001**, *123*, 7433−7434.
(67) Mirkin, N. G.; Krimm, S. *J. Phys. Chem. A* **2002**, *106*, 3391−3394.
(68) Lord, R. C. *Appl. Spectrosc.* **1977**, *31*, 187−194.
(69) Mikhonin, A. V.; Bykov, S. B.; Lednev, I. K.; Asher, S. A. In preparation, 2004.
(70) Torii, H.; Tatsumi, T.; Tasumi, M. *J. Raman Spectrosc.* **1998**, *29*, 537−546.
(71) Chi, Z.; Chen, X. G.; Holtz, J. S. W.; Asher, S. A. *Biochemistry* **1998**, *37*, 2854−2864.

Table 1. Temperature Dependence of Amide UV Raman Bands for Different Unfolded (Non-α-Helical) Polypeptides Compared to That of PPII Helical XAO Peptide

	XAO-peptide (>80% PPII helical) neutral pH		Ala_5-Ala_3 "random coil" neutral pH		AP, non-α-helical neutral pH		unfolded Apo-Mb (<20% α-helix) pH = 1.86	
	$d\nu/dT$	$\nu_{60\,°C}$, cm^{-1}	$d\nu/dT$	$\nu_{50\,°C}$, cm^{-1}	$d\nu/dT$	$\nu_{60\,°C}$, cm^{-1}	$d\nu/dT$	$\nu_{56\,°C}$, cm^{-1}
AI	0.02 ± 0.01	1659	0.052 ± 0.02	1667	0.052 ± 0.02	1659	0.06 ± 0.01	1671
AII	-0.14 ± 0.01	1545	-0.14 ± 0.01	1558	-0.14 ± 0.01	1548	-0.17 ± 0.04	1550
$C_\alpha H_{(1)}$	0.008 ± 0.016	1388	-0.015 ± 0.02	1397	-0.015 ± 0.02	1399	-0.02 ± 0.04	1393
$C_\alpha H_{(2)}$	0.018 ± 0.017	1365	-0.01 ± 0.02	1373	-0.01 ± 0.03	1377 broad	N/A	1378 broad
$AIII_2$	-0.03 ± 0.02	1300	-0.03 ± 0.01	1305	-0.03 ± 0.01	1311	-0.05 ± 0.04	1295
$AIII_3$	-0.10 ± 0.02	1241	-0.094 ± 0.018	1250	-0.094 ± 0.018	1247	-0.11 ± 0.03	1240

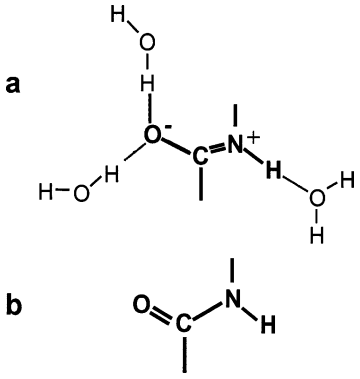

Figure 3. Resonance forms of amide peptide bond. Hydrogen bonding stabilizes resonance form a, which stabilizes C−O single bonding and C=N double bonding.

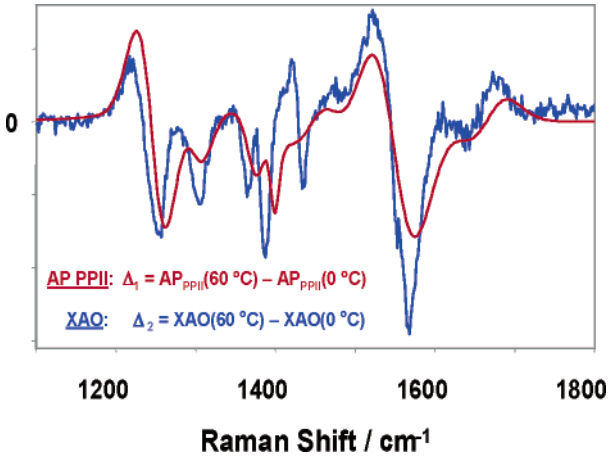

Figure 4. UV Raman difference spectra between +60 °C and 0 °C for the PPII conformation of XAO and that of AP.

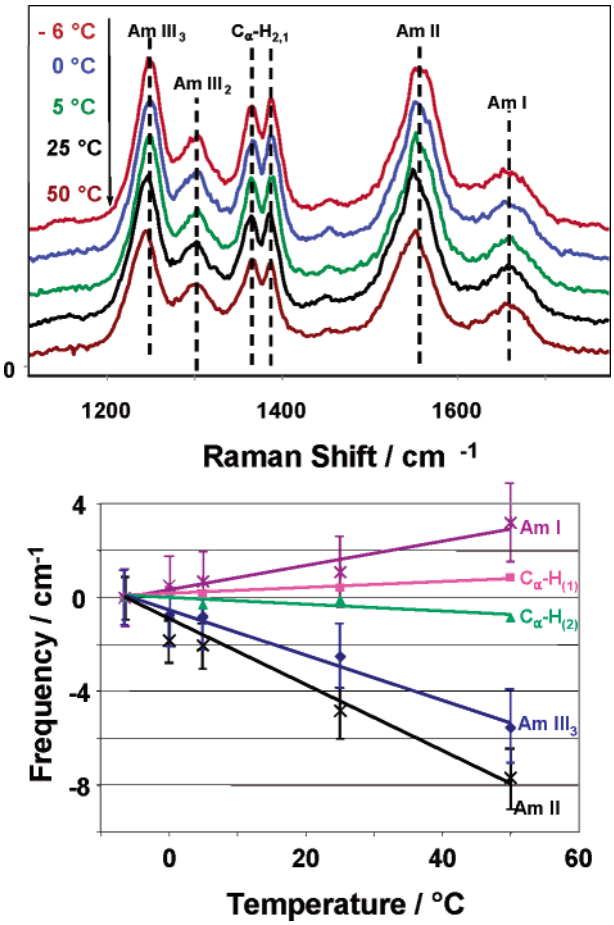

Figure 5. Temperature dependence of $A_5 - A_3$ 204-nm Raman difference spectra and temperature dependence of the $A_5 - A_3$ amide band frequencies.

Φ-angles spanning a broad region of angles within the Ramachandran dihedral angle plane.

We could use these spectral data to determine the range of Ψ- and Φ-angles if we knew the homogeneous line width of the $AmIII_3$ bands and the dependence of the center frequencies on the Ψ- and Φ-angles. We can estimate the intrinsic homogeneous line width of the bands from UV Raman spectra of crystals of peptides.

Determination of Amide Band Homogeneous Line Width. Figure 7 shows the 229-nm Raman spectra of a powder of Gly-Ala-Leu trihydrate crystals grown out of a methanol−water mixture[72] (for which we have also determined a crystal structure). In addition, Figure 7 shows the Raman spectrum of a powder of Gly-Ala-Leu directly out of the Bachem Company bottle. This powder is claimed by Bachem to result from drying an aqueous solution of Gly-Ala-Leu.

The X-ray diffraction crystal structure[72] of this Gly-Ala-Leu-trihydrate crystal shows that the Ala-Leu peptide bond has α-helix-like Φ- and Ψ-angles (−67°, −40°). As expected, the Raman spectrum of the trihydrate crystal shows a high-frequency, sharp α-helix-like Am III_3 band at 1292 cm^{-1}. The Gly-Ala-Leu powder from Bachem shows a similar sharp $AmIII_3$ band, which is shifted 50 cm^{-1} to lower frequency. We do not know the peptide structure in this powder. However, the $AmIII_3$ frequency is consistent with a more planar *β*-strand-like or PPII-like conformation.

Since the trihydrate crystal shows a single well-defined hydrogen bonding geometry, the observed Raman bandwidths

(72) Chaturvedi, S.; Go, K.; Parthasarathy, R. *Biopolymers* **1991**, *31*, 397−407.

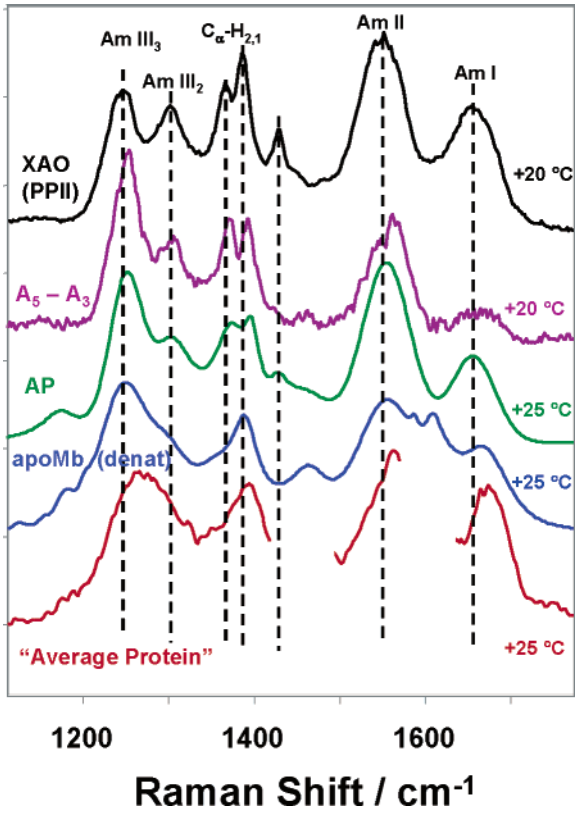

Figure 6. Comparison of 204-nm PPII helical XAO spectrum (+20 °C) to the spectra of non-α-helical structures for different peptides and proteins: $A_5 - A_3$ (+20 °C), AP (+25 °C), acid-denatured apoMb (pH = 1.86, +25 °C), "average protein" (+25 °C). The "average protein random coil" spectrum is the average UV Raman spectrum obtained for non-α-helical and non-β-sheet secondary structures in a library of 13 native proteins.[71]

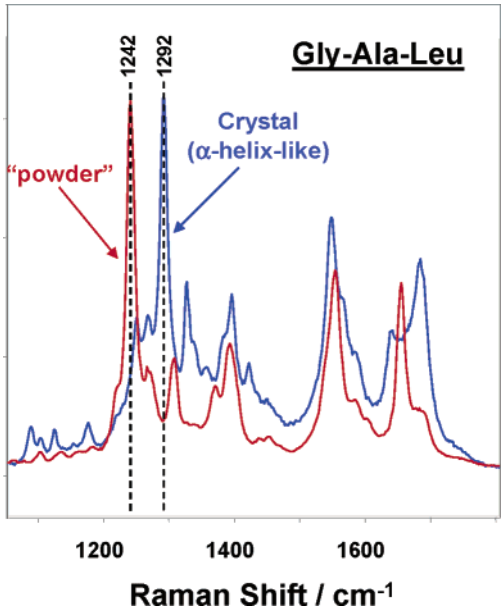

Figure 7. Comparison of 229-nm Raman spectrum of crystal Gly-Ala-Leu·3H_2O ({Ψ,Φ} = {-40°,−67°}) to that of "powder" Gly-Ala-Leu.

should be close to that of the homogeneous line width of the Raman band (assuming identical dephasing rates in the crystal and in solution). Both the trihydrate crystal and the Bachem powder show $AmIII_3$ bandwidths of 15 cm^{-1} (full width at half-height). This bandwidth is significantly larger than our spectral resolution of 6 cm^{-1}. Thus, assuming a Lorentzian band shape we calculate 7.5 cm^{-1} homogeneous line widths. The fact that the Bachem powder shows a similar narrow bandwidth indicates that the peptide also occurs in a single well-defined conformation in this powder environment.

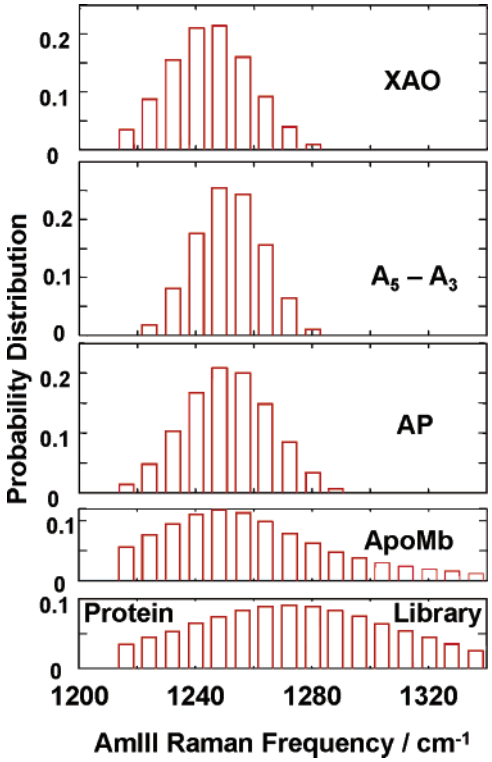

Figure 8. Deconvolution of homogeneously broadened $AmIII_3$ Raman band shape from Figure 7 of XAO, $A_5 - A_3$, non-α-helical AP, acid-denatured apoMb, and "disordered" protein conformations. The resulting histogram shows the population distribution associated with the plotted $AmIII_3$ frequencies.

Deconvolution of $AmIII_3$ Frequency Distribution for Non-α-Helical States of Peptides and Proteins. Given this homogeneous line width, we can very roughly estimate the distribution of Ψ-angles by neglecting the dependence of the $AmIII_3$ frequencies on the Φ-angle. Previous works by both us and others have shown a much smaller AmIII band frequency dependence on the Φ-angle than on the Ψ-angle.[65−67] Further, only a very limited region of Φ-angles can be populated because of steric constraints. We note that our argument also neglects the unlikely possibility that major contributions occur from Φ-angles, which occur in the left-handed α-helix conformation.

We assume that the inhomogeneously broadened experimentally measured $AmIII_3$ band profile, $A(\nu)$, is the sum of M single Lorentzian bands with identical homogeneous line widths, Γ, with different center frequencies, νe_i:

$$A(\upsilon) = \pi^{-1} \sum_{i=1}^{M} L_i \cdot \frac{\Gamma^2}{\Gamma^2 + (\upsilon - \nu e_i)^2} \qquad (1)$$

where L_i is the probability for a band to occur at frequency νe_i. We deconvoluted the measured XAO, AP, acid-denatured apoMb, and average disordered protein spectra into their population distributions of identical 7.5 cm^{-1} Lorentzians. Figure 8 shows histogram plots of the underlying spectral probability distributions. $A_5 - A_3$ shows the narrowest distribution of

frequencies, while the "protein library" shows the broadest. AP is similar to XAO except that it is shifted to higher frequency. Acid-denatured apoMb shows a broad range of frequencies; however, it shows a significant maximum around the PPII frequencies.

These deconvolutions also assume that the Raman cross sections of these bands are independent of frequency (i.e., Ψ-angle independent). This is a reasonable assumption, since the only major amide band cross section dependence observed, to date, is for the α-helix conformation, which appears to result from hypochromic α-helix excitonic interactions by the resonance electronic transitions.[54,55,73−76] This cannot occur here because no extended α-helices contribute, and each amide bond scatters independently.[77,78] The only possible Raman cross section dependence would occur in the presence of a large normal mode composition dependence on the band frequency.

Quantitative Correlation of Ψ and the AmIII$_3$ Frequency. We previously used Gaussian 98W to calculate the Ψ-dihedral angle dependence of the amide III frequency of alanine methylamide in a vacuum.[65] The frequency dependence was carried out by fixing Ψ at the angles of interest and then optimizing the geometry of the peptide at each angle. The vibrational frequencies were determined for each optimized geometry. We found a sin Ψ-dependence: $\upsilon = \upsilon_o + A \sin(\Psi + a)$.

This equation is likely to only roughly estimate the correlation between the AmIII$_3$ frequency and the Ψ-angle. However, it appears to capture the physics of the frequency dependence in that it calculates the Ψ-angular dependence of the coupling of the AmIII$_3$ vibration with C_α−H bending. It predicts a sinusoidal relationship which correlates with the projection of N−H and C_α−H sb motion. The parameters found from the theoretical fit can be made more predictive for peptides in water by refitting this equation to experimental data for peptide bonds at known Ψ-angles. Thus, we fit the expression to three points: the α-helix-like peptide Gly-Ala-Leu-trihydrate with $\Psi = -40°$ and $\nu_{III3} = 1292\ cm^{-1}$, the XAO peptide in water in the PPII state with $\Psi = 145°$ and $1242\ cm^{-1}$, and poly-L-lysine, poly-L-glutamic acid mixture (which forms a β-sheet),[69] with $\Psi = 120°$ and $1227\ cm^{-1}$. We obtain:

$$\upsilon = 1265\ cm^{-1} - 46.8\ cm^{-1} \sin(\Psi + 5.2°) \qquad (2)$$

We can then use eq 2 to analyze Figure 8 to roughly estimate the Ψ-angle distribution of our peptides and proteins (Figure 9).

We are aware that Mirkin and Krimm[67] calculations show a significant dependence of the AmIII band frequency on the Φ-angle. They point out that this dependence will tend to confound a simple correlation relationship such as eq 2, proposed here. However, the Ψ-dependence still generally dominates the Ψ-, Φ-dependence. The relationship in eq 2 derives from a theoretical dependence that captures the physics of the coupling of C_α−H and N−H motions, which is then empirically fit to spectral data for particular known conformations. The proposed relationship is likely to span the region of the β-sheet, PPII, and α-helical conformations discussed here and lead to rough estimates of Ψ-angles.

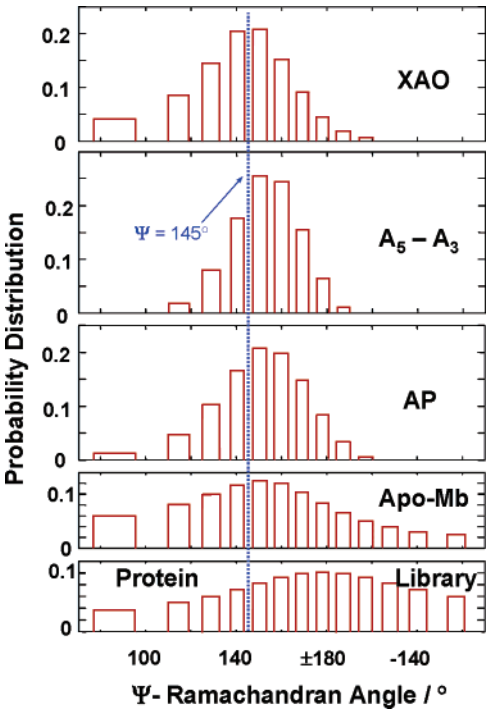

Figure 9. Estimated Ψ-Ramachandran angle distribution of XAO, $A_5 - A_3$, non-α-helical AP, acid-denatured apoMb, and "disordered" state of an "average protein" (from a library of folded proteins).

Our approach here is used to estimate the correlation between the AmIII frequency and the Ψ-angle. For AP we find $\Psi = 152 \pm 26°$. The distribution in Ψ suggests significant population of β-strand conformations. This would be consistent with Sreerama and Woody's molecular dynamics calculation of A_8,[79] which indicated that each amide bond populates both the PPII and β-strand conformations. However, the β-strand was found to be 2- to 3-fold less populated than the PPII conformation.

The Ψ-angle distribution found for the non-α-helix and non-β-sheet protein library spectrum indicates that a large range of Ψ-angles are populated (80−180° and −180° to −120°). These include even angles outside the normally allowed range of $40° < \Psi < 180°$ and $-180° < \Psi < -160°$ for unconstrained amide bonds. This large range of amide bonds Ψ-angles is expected since the folded protein structures utilize packing constraints to force these unusual dihedral angles.

Transient Melting of AP α-Helix to PPII. Figure 10, which was adapted from Figure 3 of Lednev et al.,[47] shows the time dependence of the UVRS spectral changes induced by a T-jump between 4 and 35 °C for AP in water. We can now interpret these data in terms of α-helix → PPII transition, rather than to a random coil conformation. A careful measurement of the frequency of the difference peak finds it identical to that in the steady-state spectrum (top), indicating the dominant conformation is to a state with $\Psi = 150°$, almost certainly PPII.

At short delay times (≤40 ns) we only see features which are due to changes in the temperature-dependent hydrogen bonding strength between PPII AP and water. These spectral

(73) Schellman, J. A.; Becktel, W. J. *Biopolymers* **1983**, *22*, 171−187.
(74) Momii, R. K.; Urry, D. W. *Macromolecules* **1968**, *1*, 372.
(75) Onari, S. *Jpn. J. Appl. Phys.* **1970**, *9*, 227.
(76) Moffit, W. *Proc. Natl. Acad. Sci. U.S.A.* **1956**, *42*, 736.
(77) Mix, G.; Schweitzer-Stenner, R.; Asher, S. A. *J. Am. Chem. Soc.* **2000**, *122*, 9028−9029.
(78) Mikhonin, A. V.; Asher, S. A. In preparation, 2004.
(79) Sreerama, N.; Woody, R. W. *Proteins: Struct., Funct., Genet.* **1999**, *36*, 400−406.

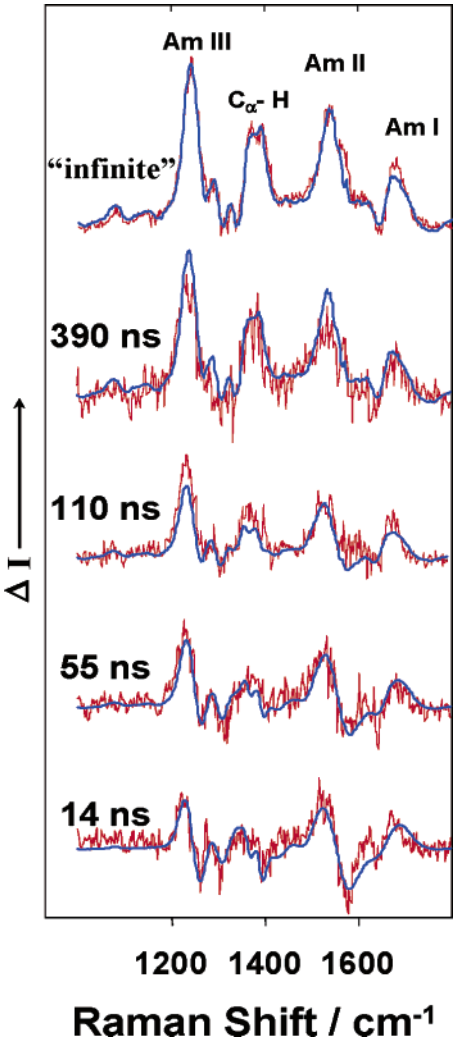

Figure 10. AP UVRS spectrum (top curve) measured in H_2O at 4 °C and transient difference UVRS of AP solution initially at 4 °C at different delay times after T-jump of ~31 °C. The steady-state difference UVRS spectrum between 35 and 4 °C is equivalent to the transient difference spectrum at infinite delay time. Adapted from Figure 3 of Lednev et al.[47]

changes are not associated with the α-helix → PPII conformational transition.[47] These features show up immediately after the IR heating pulse, and they stay constant until α-helix melting (discussed below) begins at longer delay times (≥50 ns) in the AP difference spectra. These short delay time spectral changes are identical to the difference spectra shown in Figure 4.

It was shown earlier[46,47] that the 1236, 1374, 1534, and 1678 cm^{-1} difference spectral features are contributed by the population of AP non-α-helical conformations. We now conclude that these spectral features derive from PPII conformations. The relative contributions of PPII conformations increase in the difference spectra at delay times longer than 40−50 ns. At ~400 ns, the spectral evolution is complete, and the difference spectra becomes identical to all the difference spectra at longer delay times, as well as to steady-state difference spectrum between 4 and 35 °C, which can be considered as a difference spectrum with an "infinite" delay time.

Conclusions

Numerous groups recently demonstrated the occurrence of PPII conformations in large and small peptides. We verified these conclusions for small peptides as well as for a 21-residue mainly Ala peptide, which exists below room temperature as a mixture of α-helix and PPII helix. AP is mainly in an α-helix conformation at 0 °C and is mainly in a PPII conformation above room temperature. AP undergoes a thermal melting transition between the α-helix and a PPII conformation without any evidence of other significantly populated intermediates. This is a distinctly different transition than envisioned by previous theoretical methods, which considered a melting transition from an ordered α-helical state to a disordered state.

We developed a method to estimate the Ramanchandran Ψ-angle from the AmIII frequency of peptide bonds in water solution. This has allowed us to estimate the Ψ-angle distribution in small and large peptides and in acid-denatured apoMb. We also estimated the distribution of Ψ-angles in disordered regions of folded proteins. As expected, we find population of Ψ-angles in the disordered amide bonds of folded proteins that are normally disallowed for unconstrained peptide bonds.

Acknowledgment. We would like to thank Dr. Lednev, Zeeshan Ahmed, Dr. Murza, and Bhavya Sharma for helpful and useful discussions as well as NIH Grant 8R01 EB002 053021 for financial support.

JA049518J